Molded plasmonic crystals for detecting and spatially imaging surface bound species by surface-enhanced Raman scattering

Alfred J. Baca,[1] Tu T. Truong,[1] Lee R. Cambrea,[2] Jason M. Montgomery,[3] Stephen K. Gray,[3] Daner Abdula,[4] Tony R. Banks,[1] Jimin Yao,[4] Ralph G. Nuzzo,[1] and John A. Rogers[1,4,a)]

[1]*Department of Chemistry, Fredrick Seitz Materials Research Laboratory, Beckman Institute, University of Illinois at Urbana-Champaign, Urbana, Illinois 61801, USA*
[2]*Department of Chemistry, Naval Air Warfare Center Weapons Division, China Lake, California 93555, USA*
[3]*Center for Nanoscale Materials, Argonne National Laboratory, Argonne, Illinois 60439, USA*
[4]*Departments of Material Science and Engineering and Electrical and Computer Engineering, University of Illinois at Urbana-Champaign, Urbana, Illinois 61801, USA*

(Received 5 May 2009; accepted 23 May 2009; published online 17 June 2009)

This report introduces a type of plasmonic crystal that consists of metal coated nanostructures of relief molded on a polymer film as a substrate for surface-enhanced Raman scattering (SERS). Such crystals exhibit SERS enhancement factors of $\sim 10^5$, over large areas and with sufficiently high levels of uniformity for precise two-dimensional Raman mapping of surface bound monolayers. The ease of fabrication together with the high sensitivities and spatial resolution that can be achieved suggests an attractive route to SERS substrates for portable chemical warfare agent detection, environmental monitors, noninvasive imaging of biomolecules, and other applications. © *2009 American Institute of Physics*. [DOI: 10.1063/1.3155198]

Recent advances in nanofabrication and theoretical modeling enable the design of various plasmonic nanostructures for important applications in biosensing,[1] nanophotonics,[2] and metamaterials.[3] The phenomena underlying operation of these devices are also intimately related to surface-enhanced Raman scattering (SERS).[4] The simplest and earliest SERS substrates used roughened metal films.[5] More recent work exploits deterministic nanostructures composed of metal nanoparticles and nanowires,[6,7] as well as nanoholes[8] and nanovoids[9] in metal films, and more complex structures,[10] all of which can yield SERS with reproducible high levels of sensitivity. For a given metal, areal coverage, uniformity, structural feature sizes and shapes determine the performance and modes of use. These aspects are all defined by the techniques for fabricating these structures. Despite previous important work on nanostructures for SERS, there is value in the development of large area, planar SERS substrates that can be reproducibly fabricated in cost effective ways, with spatially uniform amplification that can be engineered for operation at different wavelengths.

Here, we report quasi-three-dimensional plasmonic crystals[1,11] formed by soft lithography as SERS substrates. Experimental and computational studies of the scaling of SERS amplification factors with characteristic geometries of these crystals reveal key features of the physics. Full, two-dimensional (2D) imaging of patterned monolayers illustrates a useful operational capability enabled by the high levels of spatial uniformity that can be achieved. These well controlled, low cost, and easily fabricated substrates, together with the design rules that determine their operation, suggest a strong potential for engineered, practical use in various sensing and imaging applications.

The plasmonic crystals that served as SERS substrates were formed with a simple, soft lithographic molding technique[4] to define a pattern of relief in a layer of a photocurable epoxy (SU8, Microchem Corp.). Blanket evaporation of a thin layer of Au (~40 nm) on top of this structure completed the fabrication. The substrates studied here supported sixteen individual 4×4 mm^2 patterned regions, each composed of films of Au with square lattices of holes and recessed circular disks of Au (with some residual Au on portions of the sidewalls of the relief features). The periodicities (P) ranged from 0.49 to 1.75 μm, with corresponding diameters (D) from 0.17 to 1.12 μm. The depths of the recessed regions were ~360 nm in all cases. Figure 1(a) provides a cross-sectional schematic illustration. Figures 1(b) and 1(c) present scanning electron micrographs of a representative region and a tilted view of an individual hole, respectively. Figure 1(d) shows an optical image of an entire substrate.

The SERS spectra were collected with a Nicolet Almega XR dispersive Raman microscope (Thermo Electron Corp. Madison, WI) using a 785 nm excitation laser. To evaluate the SERS response, Au coated plasmonic crystal substrates were immersed in a 15 mM solution of benzenethiol (BT) (99.99%, Aldrich) diluted in ethanol (200-proof) for 24 h and then rinsed thoroughly with ethanol. Figure 2(a) shows transmission spectra recorded from two different patterned regions and one unpatterned area. The peak labeled A in the transmission spectra corresponds to a localized surface plasmon resonance (LSPR) with intensity concentrated at the rims of the nanowells.[11] We used three-dimensional finite-difference time-domain (3D-FDTD) simulations[12] on structures with layouts that match the experimental systems to predict the expected SERS enhancement factors. Figure 2(b) contains a plot of the electric field intensity $|E|^2$ at LSPR condition, for the substrate with $P=0.760$ μm and $D=0.514$ μm. This result shows the maximum SERS enhancement and the spatial distribution, which is localized around sections of the rim of the nanowell features.

Figure 3(a) shows a set of representative SERS spectra collected from 100–3500 cm^{-1}. The spectra for any given

a)Electronic mail: jrogers@illinois.edu.

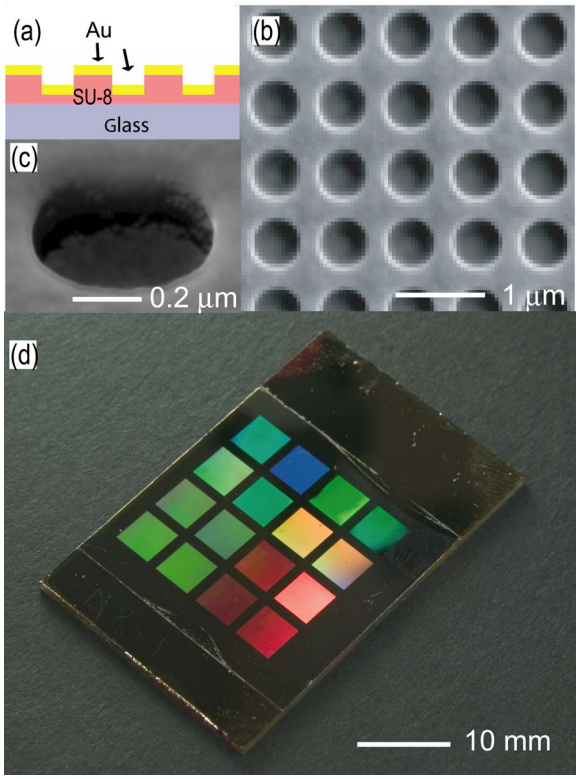

FIG. 1. (Color online) (a) Schematic cross-sectional view of a molded plasmonic crystal for use as a SERS substrate. (b) SEM image of a representative plasmonic nanoarray (D=0.514 μm, P=0.760 μm, and a depth of 0.360 μm). (c) High resolution SEM image of a single nanohole. (d) Optical image of a completed SERS substrate.

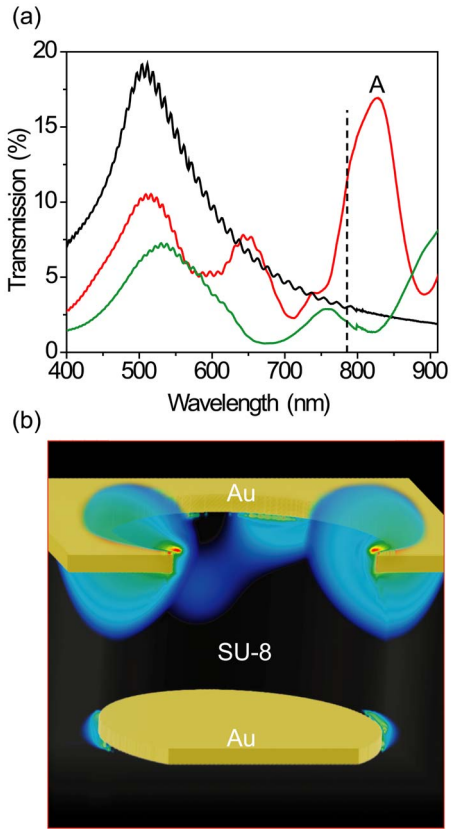

FIG. 2. (Color online) (a) Transmission spectra of flat Au (top; black) and Au coated nanoholes with (middle; red) D=0.514 μm; P=0.760 μm and (bottom; green) D=0.689 μm; P=1 μm. Dotted line corresponds to the excitation wavelength. (b) Calculated electric field intensity at 821 nm for D=0.514 μm, P=0.760 μm.

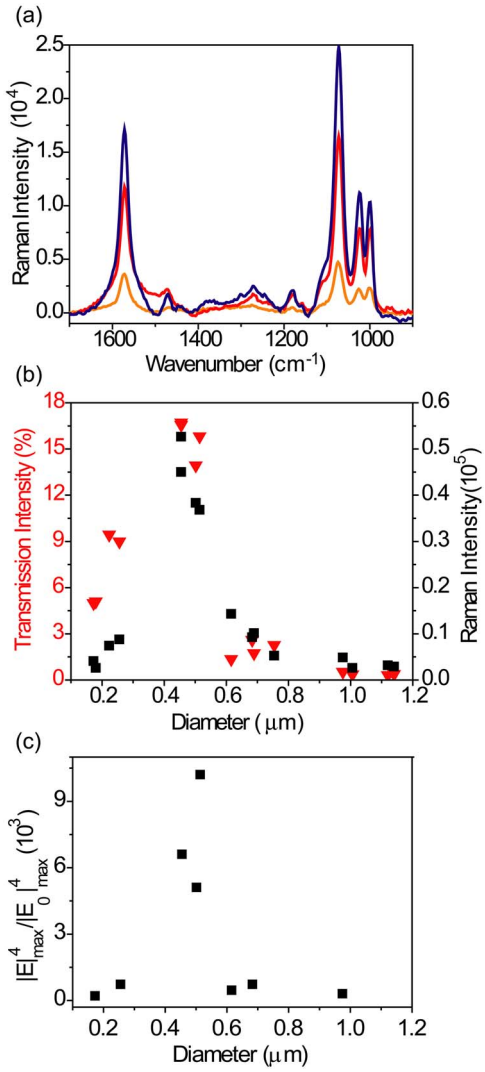

FIG. 3. (Color online) (a) SERS spectra of BT adsorbed onto areas of a molded SERS substrate composed of square lattices of cylindrical holes with different diameters (d). Blue; D=0.514 μm, red; D=0.689 μm, orange; D=1.06 μm. (b) Transmission intensity at 821 nm and SERS response as a function of D. (c) Computed electromagnetic SERS enhancement as a function of D.

array showed absence of a thiol Raman signature peak (i.e., −SH band) at around 2500 cm^{-1}, suggesting that only a monolayer of BT was formed. The results, which reveal the dependence of the response on the geometry of the crystal, is in good agreement with previously published results.[8] We attribute the SERS effect to the well known electromagnetic mechanism, predominately from the electric field localization around the rims of the nanowells. Spectra such as these exhibited high levels of spatial uniformity, with standard deviations of the intensity of the feature at ~1073 cm^{-1} of <5% for spectra recorded at different positions across 0.65 mm^2 area of the crystal (D=0.514 μm, P=0.760 μm).

The analytical enhancement factor (AEF) (Ref. 13) is defined as

$$\mathrm{AEF} = \frac{I_{\mathrm{SERS}}/C_{\mathrm{SERS}}}{I_{\mathrm{RS}}/C_{\mathrm{RS}}}, \tag{1}$$

where I_{SERS} and I_{RS} correspond to the Raman signal of a particular vibrational mode of SERS and that of the ordinary Raman spectra, respectively; C_{SERS} and C_{RS} correspond to

the number of molecules exposed to the optical excitation source for the SERS and that of the concentration in the bulk solution. Modest enhancements factors from 10^4 and 10^5 (for the band at 1073 cm^{-1}) can be achieved on these unoptimized substrates and are comparable to those obtained from similar nanostructures fabricated by serial processing techniques.[8] These enhancements vary in a systematic fashion with the crystal periodicity, diameter, depth, and λ_{exc}. Figure 3(b) shows the intensity of the Raman feature at 1073 cm^{-1} for all sixteen regions of a single SERS substrate, plotted as a function of D. Structures with $D=0.514$ μm (LSPR=826 nm) yielded the highest SERS response, which agrees with an expectation that the maximum enhancement should occur when the wavelength of the LSPR (λ_{LSPR}) is equal to the average of λ_{exc} and the wavelength of the Raman signal (λ_{RS}).[6] This condition corresponds to $\lambda_{LSPR} \sim 821$ nm. To yield additional insights, we plot the transmission at 821 nm in Fig. 3(b). The results show a clear correlation between the strength of the associated plasmonic resonance and the SERS intensity. 3D-FDTD simulations predict a similar trend, for incident light 821 nm, (electromagnetic) SERS enhancement factors $|E|^4_{max}/|E_0|^4_{max}$, where $|E_0|$ and $|E|$ are the magnitudes of the incident and calculated local electric fields, respectively, at a height 4 nm above the Au film. Figure 3(c) shows the computed response as a function of D. These results are in good accord with experiment, thereby confirming the underlying mechanisms for enhancement and suggesting a route to optimization of structure geometries.

These substrates show stable SERS response (stored in air) over a testing period of ~150 days. Molded plasmonic crystal sensors can be formed on a variety of surfaces, ranging from semiconductor wafers, for possible integration with light sources or detection electronics, to glass plates or even low cost sheets of plastic. The highly uniform nature of the crystals enables direct, spatial imaging of SERS signals. To demonstrate this possibility, we attempted two different strategies for imaging monolayers of BT. In the first, we photodefined a pattern into the SU8 imprinted plasmonic crystal composed of the letters "UIUC" (3 μm width; 10 μm long) and in the second, 1-octadecanethiol (ODT) monolayer was patterned on plasmonic crystals using microcontact printing (μCP), via a structured PDMS stamp "inked" with a 2 mM ethanolic solution of ODT which was brought into contact with the plasmonic crystal. In each case, the patterned samples were immersed in a 15 mM BT solution for 3 min prior to imaging. Figure 4(a) shows an optical image of the photopatterned UIUC letters, where in this sample only the UIUC letters contain molded nanowell features, while Fig. 4(b) shows an SEM image of the μCP patterned substrate. The lighter regions in Fig. 4(b) correspond to the ODT printed regions. Figures 4(c) and 4(d) depict the resulting 2D map of the Raman intensity at 1073 cm^{-1}, thereby revealing the spatial distribution of the patterned BT for the samples in Figs. 4(a) and 4(b), respectively. SERS imaging of pattern molecules based on metal films has been reported.[14] In contrast to previously published work, these results show good enhancement uniformity over large areas and short acquisition times (i.e., 1 s).

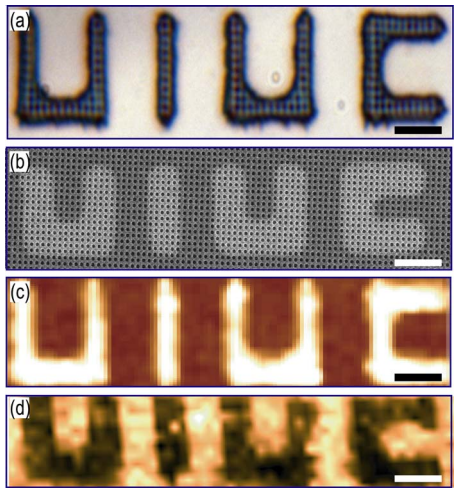

FIG. 4. (Color online) (a) Optical micrograph and (b) SEM image of photodefined and microcontact printed plasmonic crystal substrates. SERS images obtained from photodefined (c) and microcontact printed (d) BT monolayers. Ligher areas correspond to higher Raman intensity. Scale bar is 5 μm.

In conclusion, we report a simple and easy to use fabrication strategy for SERS substrates that offer highly uniform and reproducible response. The scalability of the fabrication approach to large areas, its ease of applicability with various substrates, combined with an ability to engineer the SERS response suggests a promising route to high performance SERS substrates.

A.J.B. thanks C. Conway and D. Stevenson and support from the SMART fellowship program. This work was supported by the U. S. Department of Energy (DoE), Division of Materials Sciences, Contract No. DE-FG02-07ER46471 and ONR ILIR program. Use of NERSC was supported by DOE Contract Nos. DE-AC02-05CH11231 and DE-AC02-06CH11357.

[1] V. Malyarchuk, M. E. Stewart, R. G. Nuzzo, and J. A. Rogers, Appl. Phys. Lett. **90**, 203113 (2007).
[2] R. F. Oulton, V. J. Sorger, D. A. Genov, D. F. P. Pile, and X. Zhang, Nat. Photonics **2**, 496 (2008).
[3] J. Valentine, S. Zhang, T. Zentgraf, E. Ulin-Avila, D. A. Genov, G. Bartal, and X. Zhang, Nature (London) **455**, 376 (2008).
[4] M. E. Stewart, C. R. Anderton, L. B. Thompson, J. Maria, S. K. Gray, J. A. Rogers, and R. G. Nuzzo, Chem. Rev. (Washington, D.C.) **108**, 494 (2008).
[5] M. Fleischmann, P. J. Hendra, and A. J. McQuillan, Chem. Phys. Lett. **26**, 163 (1974).
[6] C. L. Haynes and R. P. Van Duyne, J. Phys. Chem. B **107**, 7426 (2003).
[7] A. Tao, F. Kim, C. Hess, J. Goldberger, R. He, Y. Sun, Y. Xia, and P. Yang, Nano Lett. **3**, 1229 (2003).
[8] A. G. Brolo, E. Arctander, R. Gordon, B. Leathem, and K. L. Kavanagh, Nano Lett. **4**, 2015 (2004).
[9] J. J. Baumberg, T. A. Kelf, Y. Sugawara, S. Cintra, M. E. Abdelsalam, P. N. Bartlett, and A. E. Russell, Nano Lett. **5**, 2262 (2005).
[10] H. Ko, S. Singamaneni, and V. V. Tsukruk, Small **4**, 1576 (2008).
[11] M. E. Stewart, N. H. Mack, V. Malyarchuk, J. A. N. T. Soares, T.-W. Lee, S. K. Gray, R. G. Nuzzo, and J. A. Rogers, Proc. Natl. Acad. Sci. U.S.A. **103**, 17143 (2006).
[12] A. Taflove and S. C. Hagness, *Computational Electrodynamics: The Finite-Difference Time-Domain Method*, 3rd ed. (Artech House, Boston, 2005).
[13] E. C. Le Ru, E. Blackie, M. Meyer, and P. G. Etchegoin, J. Phys. Chem. C **111**, 13794 (2007).
[14] X. M. Yang, D. A. Tryk, K. Ajito, K. Hashimoto, and A. Fujishima, Langmuir **12**, 5525 (1996).